

# Wearable finger pad sensor for tactile textures using propagated deformation on a side of a finger: Assessment of accuracy

Shunsuke SATO, Shogo OKAMOTO, Yoichiro MATSUURA, and Yoji YAMADA

Department of Mechanical Science and Engineering  
Nagoya University, Japan

**Abstract**—Measuring the shear deformation of a finger pad during active haptic exploration of materials is important for analysis of textural sensations and development of tactile texture displays. Thus far, there has been no general methods to measure such deformations for active touch. To create a sensor system, we have been developing a new method for estimating the deformation of a finger pad based on the skin deformation propagated to the radial side of a finger tip. In this study, in order to validate the method, we compared the deformation or its acceleration of finger pad estimated on the basis of the acceleration measured at the radial side and those estimated by the shear force applied to the finger pad while exploring a few types of materials. The estimation errors for the deformations at 40–450 Hz were smaller than human discrimination thresholds, indicating that the accuracy of our method is satisfactory compared with human perceptual sensitivity.

**Index Terms**—Skin deformation, Skin impedance, Tactile sensor, Texture

## I. INTRODUCTION

Humans feel tactile sensations such as roughness, hardness, and friction by touching materials. The perceptual mechanisms while sensing material textures have not been fully understood; deformation of the skin when it comes in contact with materials and related activities of cutaneous mechanoreceptors intimately reflect texture perception. Therefore, it is important to measure deformations in the finger pad or forces applied to the finger pad to understand human perceptual mechanism and to develop a technique for tactile texture display. For example, vibrotactile techniques [1], [2], [3], [4], which are a major approach of texture displays, present virtual textures by controlling the spectrum of vibratory stimuli. These stimuli are typically based on the measurement of finger pad deformation.

However, it is difficult to measure finger pad deformation during active tracing of material surfaces. Thus far, direct measurements have been limited to visual observation of the finger pad through transparent materials [5], [6], which cannot be used for general materials. Therefore, many researchers have attempted to indirectly measure finger pad deformations through alternative methods. For example, Bensaïa et al. measured the resulting fingertip vibration while sliding on materials using a Hall-effect device and magnet attached at the finger tip [7]. Manfredi et al. measured the deformation of skin near the contact surface using a laser Doppler velocity

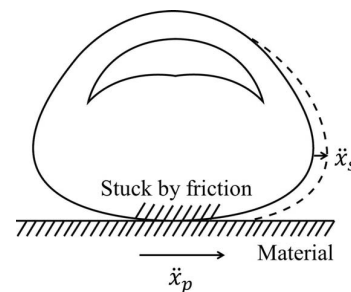


Fig. 1. Finger pad deformation and its propagation to the radial side.

meter [8]. Wiertelwski et al. measured the interaction force between the fixed finger pad and the material that slid on the finger using a high precision force sensing system [9]. Nakatani et al. estimated load on the finger pad based on the deformation of the radial finger skin by applying Poisson effect [10]. Tanaka et al. measured the skin vibration on the lateral or palmar sides of a finger using accelerometers or PVDF film attached to the finger tips [11], [12]. Okamoto et al. integrated differential outputs of two accelerometers to estimate deformation in finger pad's when a handle held by the thumb and index finger was pulled away [13]. These methods are not immediately available for measuring the finger pad's deformation under active touch. For example, some of them can be used only for passive touch where the finger and sensory apparatus are attached to each other. Furthermore, many methods did not refer to finger pad deformation but related information such as the vibration of skin adjacent to the contact part. Therefore, there is no general method, that can be used under active touch, for estimating finger pad deformation thus far.

To solve these problems, we measured the acceleration of skin deformation at the radial side, and then estimated the acceleration of finger pad deformation [14]. Through this technique, a wearable sensor for estimating shear deformation of a finger pad that can be used even under active touch can be developed because, in principle, it merely requires an accelerometer attached to the radial side of the fingertip. We confirmed that there is a high reproducibility of the relationships between the accelerations of the finger pad and its

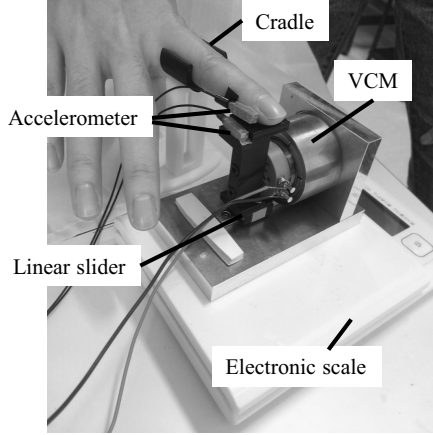


Fig. 2. Experimental apparatus for measuring accelerations at finger pad and radial side. The solid contactor was attached to the finger pad using a bonding tape. Hence, an accelerometer fixed to the contactor largely measured the acceleration at the finger pad.

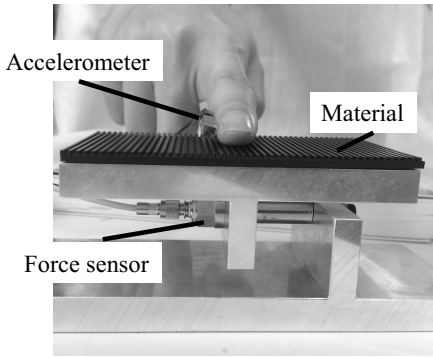


Fig. 3. Experimental apparatus for measuring the shear force applied to the finger pad and the acceleration at the radial side of a finger.

radial side for a wide frequency range. However, the accuracy of estimations was not examined in [14]. In this study, we assessed the accuracy of the estimation by comparing the estimation based on the radial skin with that based on the tangential interaction force exerted to the finger pad during active touch.

## II. PRINCIPLE: ESTIMATION OF THE FINGER PAD DEFORMATION BASED ON PROPAGATION AT THE FINGER'S SIDE

As shown in Fig. 1, the shear deformation of the finger pad induces skin deformation on the sides of a finger. Matsuura et al. [14] measured accelerations of the shear deformation of a finger pad  $\ddot{x}_p$  and radial skin  $\ddot{x}_s$ . They observed a reproducible consistency of the relationships between these two types of accelerations for a wide frequency range. They also attempted to establish a physical model of the propagation of skin deformations. However, the attempt was not successful owing to the significant individual difference of the shape of each fingertip. In the present study, we employed an approach independent from any available physical model.

If we consider that a linear relationship holds between  $\ddot{x}_p$  and  $\ddot{x}_s$  which were actually investigated later, a transfer function is defined by

$$G_1(s) = \frac{s^2 X_s(s)}{s^2 X_p(s)} = \frac{\mathcal{L}[\ddot{x}_s(t)]}{\mathcal{L}[\ddot{x}_p(t)]}. \quad (1)$$

Using this transfer function, from a sample of the skin acceleration at the side of the finger  $\ddot{x}_{s1}$ , a corresponding acceleration of the finger pad  $\ddot{x}_{p1}$  can be estimated by

$$s^2 X_{p1}(s) = s^2 X_{s1}(s) G_1(s). \quad (2)$$

## III. EXPERIMENTAL APPARATUS AND METHODS

Two subjects participated in two types of experiments. In the first experiment, the transfer function of the fingertip was specified. In the second experiment, the accuracies of estimates were compared between the two types of estimations: based on the radial skin and interaction force to the finger pad. Finger pad deformations were separately estimated from these two types of measured values and will be compared in the later section. During these two types of experiments, the subjects maintained accelerometers attached to their fingertips.

### A. Specification of transfer function between the finger pad and side

Fig. 2 shows an experimental apparatus used for specifying the transfer function between the finger pad and side. A vibration generator was used for deforming the finger pad. The vibrator drove a solid finger pad contactor which was attached to the finger pad such that slippage did not occur between the finger pad and the contactor. Hence, an accelerometer mounted on the contactor recorded the acceleration of the finger pad almost accurately. Furthermore, the finger PIP joint was fixed using a cradle to regulate the joint movement. The acceleration at the side of the finger was measured using an accelerometer attached to the radial skin of the fingertip. The measured accelerations depend on the attached position. Therefore, the specified transfer function also involves the effects of position. Both accelerations were sampled at 8 kHz. The sinusoidal vibration was within the range of 1–500 Hz. During a single measurement cycle, 10 sweeps were repeated; finger pressing forces were monitored and maintained at approximately 1 N.

### B. Simultaneous measurements of shear interaction force and acceleration at the radial side

For the purpose of validation, we simultaneously measured the shear force applied to the finger pad and the acceleration at the radial side of the finger tip during active exploration of several types of materials.

As shown in Fig. 3, similar to the previous measurement, the acceleration at the side of the finger side was measured using the accelerometer. The shear force to the finger pad was measured using a high precision load cell (9217A, Kistler) installed on a metal plate on which the materials were placed. The sampling frequency for the load cell and accelerometer was 8 kHz. The test materials included cotton cloth, aluminum plate, and two ABS-made grating scales with rectangle ridges

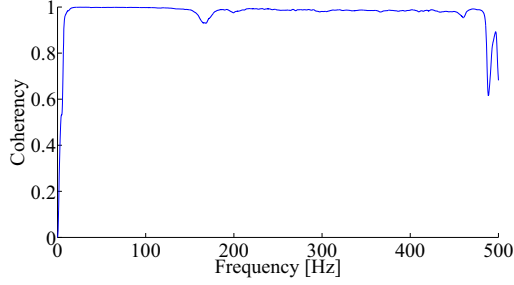


Fig. 4. Coherency between accelerations of finger pad and radial side (Subject A).

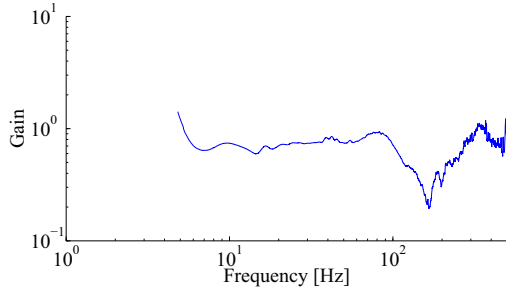


Fig. 5. Gain between accelerations of finger pad and radial side (Subject A).

of 1 mm in height and width (1 mm and 10 mm groove widths). Each subject slid a finger on the material along the sensitive direction of the load cell over a range of 50 mm with one repetition per second for a duration of ten seconds.

1) *Estimation of finger pad deformation using shear force on the finger pad:* Here, we describe how to calculate or estimate finger pad deformation under the shear force applied to it. Many earlier studies could at least in part successfully model a human finger pad as a one-d.o.f. spring and damper system when a shear force is applied to it [9], [15]. This means that a linear relationship holds between the shear deformation on the finger pad and force. Under this approximation, the equation of motion for the shear deformation of the finger pad is expressed by

$$m\ddot{x}_p(t) + c\dot{x}(t) + kx(t) = f(t) \quad (3)$$

where  $x_p(t)$ ,  $c$ ,  $k$ , and  $f(t)$  are the shear deformation of the finger pad, skin viscosity, skin elasticity, and the applied shear force, respectively. In our experimental setup,  $m$  corresponds to the effective mass of an aluminum plate.

The transfer function between  $f(t)$  and  $x_p(t)$  is

$$G_2(s) = \frac{X_p(s)}{F(s)} = \frac{1}{ms^2 + cs + k}. \quad (4)$$

For subject A,  $c$  and  $k$  were specified to be 0.21 N·s/m and 210 N/m, respectively. For subject B, these values were 0.53 N·s/m and 210 N/m, respectively. These values were close to those reported in [9] and, [15]. Using  $G_2(s)$ , the shear deformation of the finger pad  $x_p(t)$  is estimated by the shear force  $f(t)$ .

TABLE I  
MEAN ERRORS BETWEEN THE ACCELERATION ESTIMATED UNDER SHEAR FORCES ON THE FINGER PAD AND THOSE ESTIMATED ON THE RADIAL SIDE. GS STANDS FOR GRATING SCALE.

Participant	Aluminum m/s <sup>2</sup>	GS (1 mm) m/s <sup>2</sup>	Cloth m/s <sup>2</sup>	GS (10 mm) m/s <sup>2</sup>
A	$4.2 \times 10^{-3}$	$5.9 \times 10^{-3}$	$2.7 \times 10^{-3}$	$1.3 \times 10^{-2}$
B	$3.8 \times 10^{-3}$	$7.8 \times 10^{-3}$	$2.3 \times 10^{-3}$	$9.0 \times 10^{-3}$

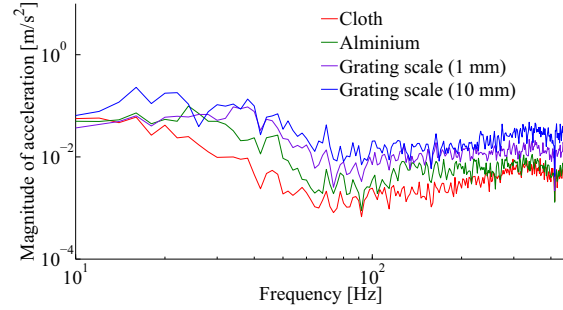


Fig. 6. Accelerations of finger pad estimated by  $G_1(s)$  (Subject A).

## IV. RESULTS

### A. Gain between the finger pad and the radial skin

Fig. 4 shows the coherency function between the accelerations on the finger pad and radial skin for subject A. The coherency was satisfactorily high at 10–450 Hz, in which the system is considered linear. In addition, the coherency for subject B exhibited a similar trend. Hence, we consider that the estimation based on the transfer function is valid for this frequency range. Fig. 5 shows the magnitude of  $G_1(s)$ , which is a gain function between the finger pad and radial skin, for subject A. The gain increased up to 80 Hz and decreased at greater frequencies with another peak around 320 Hz. The gain of subject B was not exactly same as that of subject A.

### B. Estimated accelerations of finger pad deformation

Fig. 6 shows the accelerations for the finger pad that were computed by (1) using the accelerations measured at the side of the finger. The accelerations for cloth and aluminium were relatively small whereas those for the grating scales were larger. This trend is in line with the degree of surface roughness of these four types of materials.

Figs. 7–10 show the accelerations of finger pad deformation estimated by (1) (based on radial skin) and (4) (based on shear force) when subject A explored each material. Fig. 11 shows the acceleration for the grating scale (1 mm) for subject B. Ideally, the accelerations estimated using the two different methods should match; unfortunately, this was not the case. In terms of the acceleration estimated for the radial skin (red curves), the peak commonly appeared at approximately 15 Hz for all types of materials. Around this low frequency range, the accelerations for the radial skin (red curves) were larger than those estimated by the shear forces (blue curves). In addition,

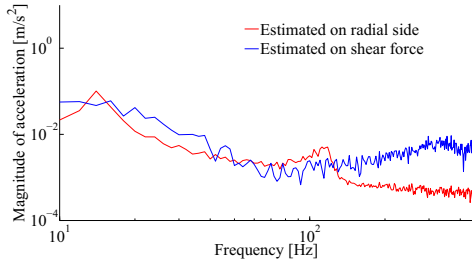


Fig. 7. Estimated accelerations on finger pad for cloth (Subject A).

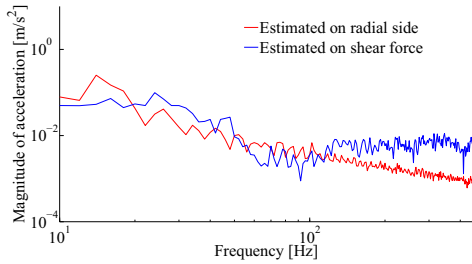


Fig. 8. Estimated accelerations on finger pad for aluminum (Subject A).

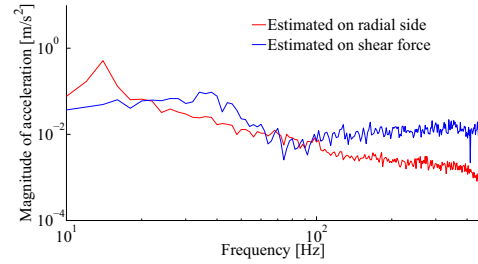


Fig. 9. Estimated accelerations on finger pad for grating scale (1 mm) (Subject A).

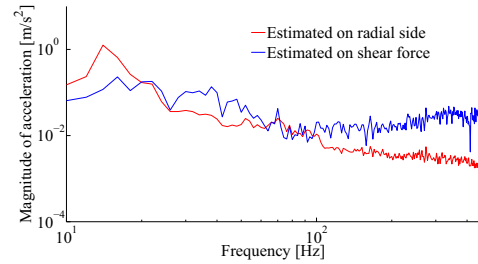


Fig. 10. Estimated accelerations on finger pad for grating scale (10 mm) (Subject A).

further discrepancies between the two methods appeared at a frequency higher than 100 Hz. We discuss the significance of these errors in the next section.

## V. DISCUSSION

Here, we discuss the significance of the errors between the two methods. Remember that we do not know that both types of estimation methods are correct. When the two types of estimates are similar, we can infer that the measured values are fairly reliable. However, when the errors are significant, we can infer that either one or both types of measurements are unreliable.

Furthermore we discuss whether or not the error is acceptable in terms of the discrimination threshold against vibrotactile stimuli. The discrimination threshold is a noticeable difference between two stimuli. In our case, this is the minimum difference of vibratory amplitudes between two pure sinusoidal vibratory stimuli that can be barely discerned. In other words, the discrimination threshold is perceptual sensitivity to physical stimuli. According to literature [16], [17], the discrimination thresholds of the magnitudes of vibrotactile stimuli are approximately 10–20% of the detection thresholds, which has been specified in [18], for a wide range of frequencies.

Table II and Fig. 12 show the mean absolute errors of finger pad deformation estimated by the radial acceleration and shear forces. The table also lists the errors of accelerations. Mean values were calculated across the materials. The discrimination thresholds were calculated on the basis of [16], [17], and [18] and are shown in Table II and Fig. 12. Their general profile is a u-shape that reaches the bottom at approximately 200–300 Hz. The mean errors between the two types of estimations were

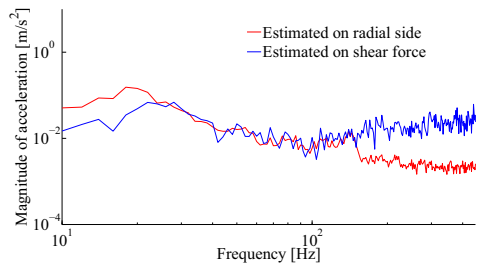


Fig. 11. Estimated accelerations on finger pad for grating scale (1 mm) (Subject B).

beneath the discrimination thresholds at high frequencies. For example, the errors between the two types of estimations were  $3.8 \times 10^{-3}$  and  $2.3 \times 10^{-3} \mu\text{m}$  for 300 and 450 Hz, respectively, and thus smaller than the discrimination thresholds. In contrast, at a few tens of Hertz, the error was comparable to the discrimination threshold. The error for 30 Hz was  $0.89 \mu\text{m}$ , which was slightly larger than the threshold of  $0.3 \mu\text{m}$ . For 15 Hz, the error between the two types of estimates was even larger ( $52 \mu\text{m}$ ). The estimation errors at low frequencies are significant.

From our comparisons between two types of measurement methods, the one using the radial skin is considered satisfactory within the frequency range of 40–450 Hz.

## VI. CONCLUSION

The future goal of this study is to realize a wearable sensor to estimate finger pad deformation while actively touching materials. Thus far, such measurement has been restricted to a

TABLE II  
MEAN ERRORS BETWEEN THE FINGER PAD'S ACCELERATIONS AND DEFORMATIONS ESTIMATED BY SHEAR FORCES AND THOSE ESTIMATED BY RADIAL SIDE'S ACCELERATIONS.

	15 Hz	30 Hz	100 Hz	300 Hz	450 Hz
Acc. err. m/s <sup>2</sup>	0.46	0.0032	0.0027	0.014	0.018
Disp. err. $\mu\text{m}$	52	0.89	$6.8 \times 10^{-3}$	$3.8 \times 10^{-3}$	$2.3 \times 10^{-3}$
Discrim. th. $\mu\text{m}$	0.4	0.25	0.04	0.013	0.022

Discrim. th. indicates the discrimination thresholds [16], [17] toward vibratory stimuli to finger pad.

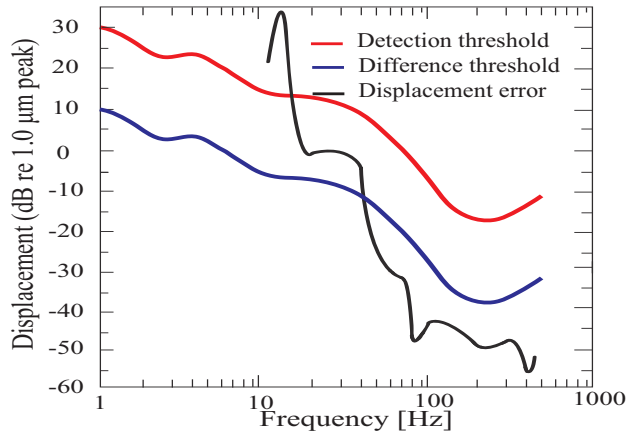


Fig. 12. Detection threshold (red) [18] and discrimination threshold (blue) against the magnitudes of vibrotactile stimuli. Estimation error of finger pad deformation between the two types of measurement methods is shown as a black curve. Estimation accuracy is considered valid at the frequency range for which the black curve is beneath the blue one.

camera-based approach using transparent materials. To achieve this goal, we use the propagation of skin deformation to the radial side in our novel approach. A linear relationship holds for a wide range of frequencies between the deformations of the finger pad and the radial skin. This enables us to estimate the deformation of one from the other. Specifically, the purpose of the present study was to validate the estimation method in terms of the estimation accuracy. For this purpose, we compared finger pad deformations estimated by our method with those estimated under shear force applied to the finger pad while four types of actual materials were explored. The estimation errors between these two methods in the frequency range 40–450 Hz were smaller than the discrimination thresholds of vibrotactile stimuli indicating that the errors are perceptually minor within this region. However, the estimation errors of the two methods were significant at lower frequencies for which further research remains to be pursued.

#### ACKNOWLEDGMENT

This study was in part supported by KAKENHI Shitsukan 25135717 and 15H05923.

#### REFERENCES

[1] Y. Matsuura, S. Okamoto, H. Nagano, and Y. Yamada, "Multidimensional matching of tactile sensations of materials and vibrotactile spectra," *Information and Media Technologies*, vol. 9, no. 4, pp. 505–516, 2014.

[2] S. Okamoto and Y. Yamada, "Lossy data compression of vibrotactile material-like textures," *IEEE Transactions on Haptics*, vol. 6, no. 1, pp. 69–80, 2013.

[3] S. Okamoto, S. Ishikawa, H. Nagano, and Y. Yamada, "Spectrum-based synthesis of vibrotactile stimuli: Active footstep display for crinkle of fragile structures," *Virtual Reality*, vol. 17, no. 3, pp. 181–191, 2013.

[4] S. Okamoto and Y. Yamada, "An objective index that substitutes for subjective quality of vibrotactile material-like textures," *IEEE/RSJ International Conference on Intelligent Robots and Systems*, pp. 3060–3067, 2011.

[5] M. J. Adams, S. A. Johnson, P. Lefèvre, V. Lévesque, V. Hayward, T. André, and J.-L. Thonnard, "Finger pad friction and its role in grip and touch," *Journal of Royal Society Interface*, vol. 10, 20120467, 2013.

[6] M. Tada and T. Kanade, "An imaging system of incipient slip for modelling how human perceives slip of a fingertip," *Proceedings of IEEE International Conference on Engineering in Medicine and Biology Society*, vol. 1, pp. 2045–2048, 2004.

[7] S. Bensmaïa and M. Hollins, "Pacian representations of fine surface texture," *Perception & Psychophysics*, vol. 67, no. 5, pp. 842–854, 2005.

[8] L. R. Manfredi, H. P. Saal, K. J. Brown, M. C. Zielinski, J. F. Dammann, V. S. Polashock, and S. J. Bensmaïa, "Natural scenes in tactile texture," *Journal of Neurophysiology*, vol. 111, no. 9, pp. 1792–1802, 2014.

[9] M. Wiertelwski, J. Lozada, and V. Hayward, "The spatial spectrum of tangential skin displacement can encode tactual texture," *IEEE Transactions on Robotics*, vol. 27, no. 3, pp. 461–472, 2011.

[10] M. Nakatani, K. Shiojima, S. Kinoshita, T. Kawasoe, K. Koketsu, and J. Wada, "Wearable contact force sensor system based on fingerpad deformation," *Proceedings of the 2011 IEEE World Haptics Conference*, pp. 323–328, 2011.

[11] Y. Tanaka, Y. Horita, A. Sano, and H. Fujimoto, "Tactile sensing utilizing human tactile perception," *Proceedings of IEEE World Haptics Conference*, pp. 621–626, 2011.

[12] Y. Tanaka, D. P. Nguyen, T. Fukuda, and A. Sano, "Wearable skin vibration sensor using a PVDF film," *Proceedings of IEEE World Haptics Conference*, pp. 146–151, 2015.

[13] S. Okamoto, M. Wiertelwski, and V. Hayward, "Anticipatory vibrotactile cueing facilitates grip force adjustment," *Proceedings of IEEE World Haptic Conference*, pp. 525–530, 2013.

[14] Y. Matsuura, S. Okamoto, and Y. Yamada, "Estimation of finger pad deformation based on skin deformation transferred to the radial side," *Haptics: Neuroscience, Devices, Modeling, and Applications. Springer Berlin Heidelberg*, pp. 313–319, 2014.

[15] N. Nakazawa, R. Ikeura, and H. Inooka, "Characteristics of human fingertips in the shearing direction," *Biological Cybernetics*, vol. 82, no. 3, pp. 207–214, 2000.

[16] J. C. Craig, "Difference threshold for intensity of tactile stimuli," *Perception & Psychophysics*, vol. 11, no. 2, pp. 150–152, 1972.

[17] G. Gescheider, S. Bolanowski, J. Zwislöcki, K. Hall, and C. Mascia, "The effects of masking on the growth of vibrotactile sensation magnitude and on the amplitude difference limen: A test of the equal sensation magnitude-equal difference limen hypothesis," *The Journal of the Acoustical Society of America*, vol. 96, no. 3, pp. 1479–1488, 1994.

[18] G. A. Gescheider, S. J. Bolanowski, and K. Hardick, "The frequency selectivity of information-processing channels in the tactile sensory system," *Somatosensory and Motor Research*, vol. 18, no. 3, pp. 191–201, 2001.